

# Particle size distribution controls the threshold between net sediment erosion and deposition in suspended load dominated flows

R. M. Dorrell<sup>1</sup>, L. A. Amy<sup>2</sup>, J. Peakall<sup>3</sup> and W. D. McCaffrey<sup>3</sup>

<sup>1</sup> Energy and Environment Institute, University of Hull, Hull, HU6 7RX, UK.

<sup>2</sup> School of Earth Sciences, University College Dublin, Dublin 4, Ireland.

<sup>3</sup> School of Earth and Environment, University of Leeds, Leeds, LS2 9JT, UK.

Corresponding author: Robert M. Dorrell (r.dorrell@hull.ac.uk)

## Key Points:

- New flow power sediment entrainment model scales with flow depth instead of particle size and incorporates capacity and competence limits.
- Suspended load, at the threshold between net erosion and deposition, is shown to be controlled by the particle-size distribution.
- Flow power model offers an order of magnitude, or better, improvement in predicting the erosional-depositional threshold.

*This is the peer reviewed version of the following article: Dorrell, R. M., Amy, L. A., Peakall, J., & McCaffrey, W. D. (2018). Particle size distribution controls the threshold between net sediment erosion and deposition in suspended load dominated flows. Geophysical Research Letters, 45, 1443–1452, which has been published in final form at <https://doi.org/10.1002/2017GL076489>. This article may be used for non-commercial purposes in accordance with Wiley Terms and Conditions for self-archiving.*

## **Abstract**

The central problem of describing most environmental and industrial flows is predicting when material is entrained into, or deposited from, suspension. The threshold between erosional and depositional flow has previously been modeled in terms of the volumetric amount of material transported in suspension. Here a new model of the threshold is proposed, that incorporates: i) volumetric and particle size limits on a flow's ability to transport material in suspension; ii) particle-size distribution effects; and iii) a new particle entrainment function, where erosion is defined in terms of the power used to lift mass from the bed. Whilst current suspended-load transport models commonly use a single characteristic particle-size the model developed herein demonstrates that particle-size distribution is a critical control on the threshold between erosional and depositional flow. The new model offers an order of magnitude, or better, improvement in predicting the erosional-depositional threshold and significantly outperforms existing particle-laden flow models.

## **1 Introduction**

When particle-laden flows erode or deposit material the fundamental properties of the flow (hydrodynamics), and through time, the surfaces over which a flow travels (morphodynamics) are changed. Therefore, whether a flow is net erosional or depositional is of key importance in environmental and industrial fluid dynamics, e.g. on: landscape erosion and evolution [*Houssais et al.*, 2015; *Bufe et al.*, 2016]; the efficiency of hydraulic engineering structures such as dams [*Yang*, 2006; *Wang et al.*, 2015]; the effectiveness of flood protection measures [*Nittrouer et al.*, 2012]; and pipe flow obstruction or erosion-corrosion [*Parsi et al.*, 2014]. Equivalent terminology may use sub-saturated flow and supersaturated flow to define if a flow is net erosional or depositional [*van Maren et al.*, 2009]. The threshold between erosion and deposition, i.e. the

condition of equilibrium in particle-laden flow, is arguably the most important prediction a sediment transport model is required to make. Hence, here we use the prediction of the threshold between net erosional and net depositional flow, as the key criterion for testing sediment transport models.

In natural flows sediments are predominately transported by turbulent fluid motion as suspended load, and material interacting with the bed (bedload) is negligible in terms of bulk sediment flux [Syvitski *et al.*, 2003]; consequently we concentrate on modeling the transport of suspended load. In keeping with most existing predictions of suspended load transport we assume low concentration, non-cohesive flow, and model the limiting threshold where sediment erosion balances deposition [Yang, 2006]. Therefore, in dilute flow, sediment concentration below or above an equilibrium value respectively defines if a flow is net erosional or depositional [van Maren *et al.*, 2009]. The test of the suspended load transport models is thus the comparison of observed versus predicted hydrodynamic and suspended load conditions at the net erosion-deposition threshold.

Common suspended load transport models are based on flow velocity, depth, concentration and a single characteristic particle size (i.e., monodisperse models [Velikanov, 1954; Bagnold, 1966; Celik and Rodi, 1991; Kubo *et al.*, 2005; Yang, 2006; Garcia, 2008; Bizzi and Lerner, 2015]), often the median particle diameter. Although suspended load transport models can show good agreement with individual sets of laboratory or field based observations, they invariably show poorer agreement when compared with other empirical datasets [Yang, 2006; Walling, 2009]. However, the particle-size distribution of sediment in natural [Bayat *et al.*, 2015] and industrial flows [Parsi *et al.*, 2014; Sajeesh and Sen, 2014] is often wide and fine-tail skewed (motivating the standard use of a log-normal particle-size scale [Soulsby, 1997; Garcia, 2008]). As has been

previously recognized particle distribution may affect sediment transport processes [*Smith and Hopkins, 1973*], thus some numerical sediment transport models use finite discretization of particle-size distributions, i.e. polydisperse models, to simulate the transport dynamics of particles of mixed sizes [*Wilcock and Southard, 1988; Armanini and Di Silvio, 1988; Garcia and Parker, 1991; McLean 1991, 1992; Blom and Parker, 2004; Strauss and Glinsky, 2012; Dorrell et al., 2013; Basani et al., 2014; Halsey et al., 2017*]. However, the effect of mixed size distributions, i.e. polydispersity, on the threshold between erosion and deposition from suspended load particle transport, and thus the effectiveness of common monodisperse models of sediment transport at the deposition-erosion threshold, has not been robustly investigated.

A further key shortcoming of most sediment transport models is that capacity and competence are not jointly considered. Capacity describes the maximum amount of material that a turbulent flow can support: i.e., capacity can be defined as the sum volumetric concentration,  $c$  (sediment volume per unit volume,  $v/v$ ), of all material in suspension at the net erosional-depositional threshold [*Dorrell et al., 2013* and references therein]. Competence describes the maximum particle size that can be transported by a flow. Although these two limits on particle transport are fundamentally related [*Dorrell et al., 2013*], most approaches to threshold calculation only incorporate one of these controls [e.g., *Shields, 1936; Kubo et al., 2005*], which reduces their effectiveness for general use.

## **2 Methods**

Here we examine the ability of existing models to describe the erosion-deposition threshold of suspended load sediment transport by comparing them to a collated empirical data set of equilibrium flow [*Vanoni, 1946; Brooks, 1954; Einstein and Chien, 1955; Vanoni and Nomicos,*

1960; *Nordin and Dempster*, 1963; *Guy et al.*, 1966; *Ashida and Okabe*, 1982; *Coleman*, 1986; *Lyn*, 1988; *Cellino and Graf*, 1999; *Graf and Cellino*, 2002]. We then introduce a new sediment transport model that incorporates polydispersity, and allows for both competence and capacity driven sedimentation, and demonstrate that this outperforms existing models.

## 2.1 Empirical Data

The collated empirical data set include flows with both narrow and wide particle-size distributions and experimental and field observations (see Supporting Data Table 1). Collected data were restricted to flat beds to avoid enhanced sediment suspension effects arising from flow over an uneven bed [*Soulsby*, 1997].

As reported in original data sources, empirical measurements collated include: depth average flow velocity,  $u$ , and shear velocity,  $u_*$ ; flow depth,  $h$ ; depth average concentration of the suspended load,  $c$ ; and the particle-size distribution at threshold conditions (see section 2.2). Original data sources use different models to determine shear velocity, i.e.: i) depth-based,  $u_* = \sqrt{ghS}$ , where  $g$  is gravity and  $S$  is bed slope [*Nordin and Dempster*, 1963; *Guy et al.*, 1966]; ii) hydraulic-radius based  $u_* = \sqrt{gR_hS}$ , where  $R_h$  is the hydraulic radius [*Vanoni*, 1946; *Einstein and Chien*, 1955; *Vanoni and Nomicos*, 1960; *Coleman*, 1986; *Lyn*, 1988]; iii) Reynolds-stress based, either derived from fitting a Rouse number to the flows' equilibrium concentration profile [*Ashida and Okabe*, 1982], or fitting the shear velocity to the shear stress profile [*Cellino and Graf*, 1999; *Graf and Cellino*, 2002]; and iv) bed-friction  $u_* = u\sqrt{f_b/8}$ , where  $f_b$  is a specified bed friction coefficient [*Brooks*, 1954]. Depth average variables were calculated by integrating empirical profiles over the height of the flow and dividing by the flow depth.

## 2.2 Particle-Size Distribution Fitting

To close both mono- and polydisperse models of the threshold between net erosional and depositional flow both a characteristic suspended-load particle size and the particle-size distribution are determined from the collated empirical data (Figures 1 and 2). Monodisperse models are closed using the median particle size,  $d_{50}$ , although other authors have used different percentile particle sizes to characterise suspended and bed load sediment transport [van Rijn, 1984a].

The collated set of empirical data of flow at the threshold between net erosion and deposition can be separated into three types based on particle size data recorded (see Figure 1 and Supporting Data Table 1):

- A. Both the initial (before use in laboratory experiments) and the suspended load size distribution are recorded [Experiments 1-7, from: *Guy et al.*, 1966].
- B. Only the size distribution of the suspended load (fluvial data) is recorded [Experiments 8-30, from: *Nordin and Dempster*, 1963].
- C. Only the initial size distribution of material before use in laboratory experiments is recorded [Experiments 31-70, from: *Vanoni*, 1946; *Brooks*, 1954; *Einstein and Chien*, 1955; *Vanoni and Nomicos*, 1960; *Ashida and Okabe*, 1982; *Coleman*, 1986; *Lyn*, 1988; *Cellino and Graf*, 1999; *Graf and Cellino*, 2002].

The type A and B empirical data may be directly used to determine an appropriate particle-size distribution. Here a skewed log-normal distribution, with a cumulative distribution function, CDF( $\phi$ ),

$$(1) \quad \text{CDF}(\phi) = \int_{-\infty}^{\phi} \left( \sqrt{\frac{2}{\omega^2\pi}} e^{-\frac{1}{2}\left(\frac{x-\xi}{\omega}\right)^2} \int_{-\infty}^{\psi\left(\frac{x-\xi}{\omega}\right)} e^{-\frac{t^2}{2}} dt \right) dx,$$

is fitted to empirical measurements of the CDF for three  $\phi$ -scale particle sizes (fine, medium and coarse). The distribution is discretised, using a  $\phi$ -scale bin size of 0.01. The location,  $\xi$ , scale,  $\omega$ , and shape,  $\psi$ , parameters are calculated by solving the resultant set of linked numerical equations using Matlab's non-linear system solver, `fsolve`, based on Powell's method [Powell, 1964]. The derived particle distribution is constrained to the central 99% region of a fitted probability function to avoid infinitely small and infinitely large particle classes.

For the type C data, a direct fit to particle size data cannot be used, as fractionation will result in change in the particle-size distribution [Whitehouse, 1995]. It is found from the type A data that the median particle size of suspended load,  $\tilde{\phi}_{50}$  (as denoted by tilde notation), is consistently equivalent to the 8<sup>th</sup> percentile of the initial distribution,  $\phi_{08}$ . This agrees with previous studies that report the median suspended load particle size as in the range of 2<sup>nd</sup> to 15<sup>th</sup> percentile of material comprising the bed [Whitehouse, 1995]. Although this fractionation rule may not hold for predominately fine-grained systems [see, e.g., Nittrouer *et al.*, 2011], the median size of the type A data ranges from  $2.97 \geq \phi_{50} \geq 2.33$  and the median (unweighted) size of the type C data is also coarse, predominantly in the range  $3 \geq \phi_{50} \geq 2$  (see Supporting Data Table 1). Thus, for the type C data only the assumed suspended load distribution is weighted, following the empirical rule determined above, to account for particle fractionation. However, scale and shape parameters are assumed unchanged in the weighted distribution. A two-stage process is thus used to determine a characteristic particle-size distribution:

- i. A fit of a skewed log-normal distribution to initial particle data to determine: the 8<sup>th</sup> percentile particle size and the scale,  $\omega$ , and shape,  $\psi$ , parameters.
- ii. A shift in the fitted skewed log-normal distribution such that  $\tilde{\phi}_{50}$  is equivalent to  $\phi_{08}$ .

The particle distribution shift in stage ii is made using Matlab's `fsolve` to find a new weighted location parameter,  $\tilde{\xi}$ , such that for the initial particle size distribution, the cumulative distribution function evaluated at,  $\phi_{08}$ , is equal to 50%, i.e.  $CDF(\phi_{08}, \tilde{\xi}, \omega, \psi) = 50\%$ .

### 3 Results

#### 3.1 Particle-Laden Flow Hydrodynamics at Equilibrium

Here the hydrodynamics of particle-laden flow at equilibrium are quantified by the dimensionless ratio of the flow force acting on stationary particles to their submerged weight: here defined as  $\Gamma = \tau^*/g\Delta\rho d_{50}$ , where  $\tau^*$ ,  $\Delta\rho = \rho_s - \rho$ , and  $d_{50}$  respectively denote shear stress (characterised by a shear velocity:  $u_*^2 = \tau^*/\rho$ ), particle-fluid density difference and median particle diameter. The dimensional critical shear velocity for incipient particle motion of a particulate bed is denoted  $u_{*c}$ . Such an approach is chosen as it allows direct comparison to the common dimensionless models of incipient motion [*Shields*, 1936] and the Rouse condition for suspended load transport [*Rouse*, 1937]. Examination of the collated laboratory and field data set of flows at the net erosional-depositional threshold shows that the hydrodynamics of the particle-laden flow at equilibrium are intrinsically related to the particle-size distribution. The dimensionless shear stress required to maintain threshold conditions increases as the particle-size distribution widens (**Figure 1**). This effect even occurs when the median particle size remains constant and thus cannot be captured by monodisperse models.

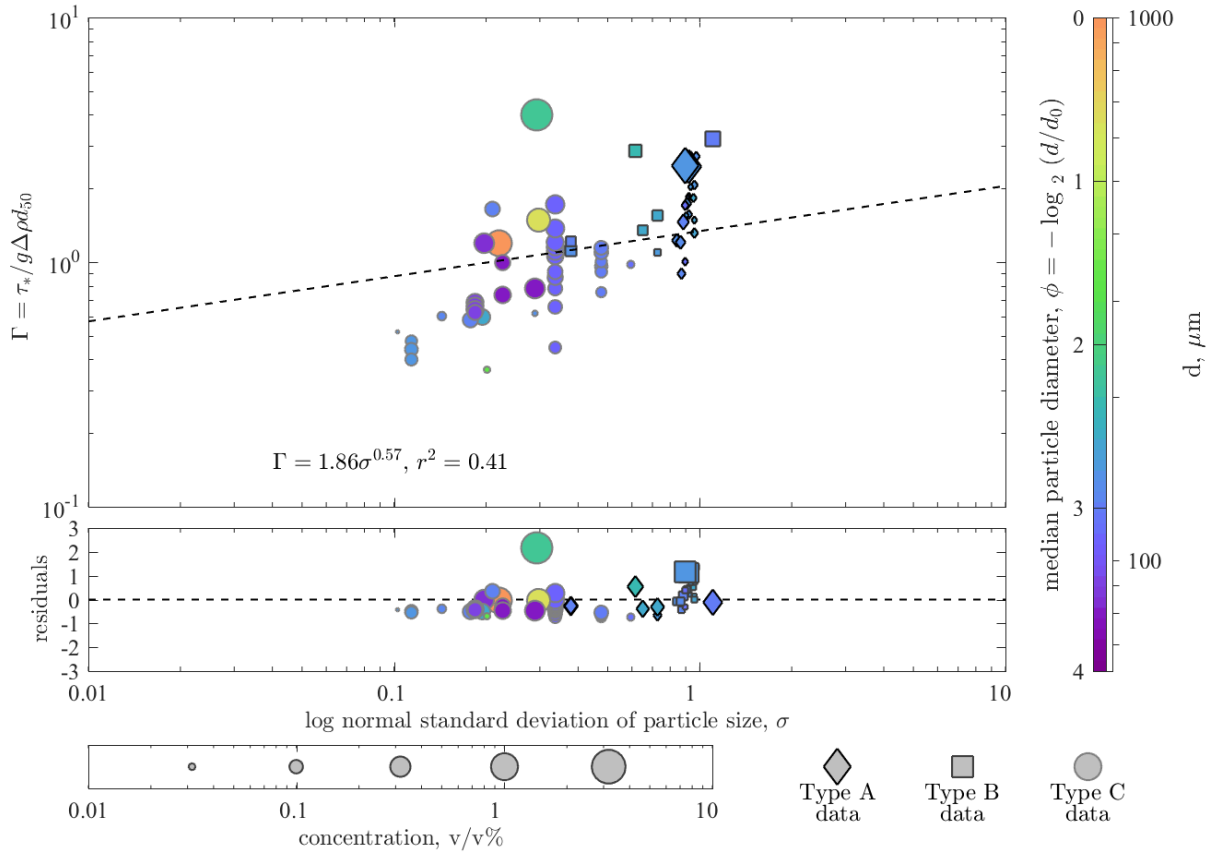


**Figure 1** Dimensionless shear stress,  $\Gamma$ , at the net erosion-deposition threshold, as a function of log normal standard deviation of the particle-size (see section 2.2). Residuals plot deviation from line of best fit. Colors denote  $\phi$ -scale median particle size, where  $\phi = -\log_2(d/d_0)$  and  $d_0 = 1$  mm. Concentration is depicted by symbol size. Empirical data types (A-C), and original sources, are defined in the methods section and in Supporting Data Table 1.

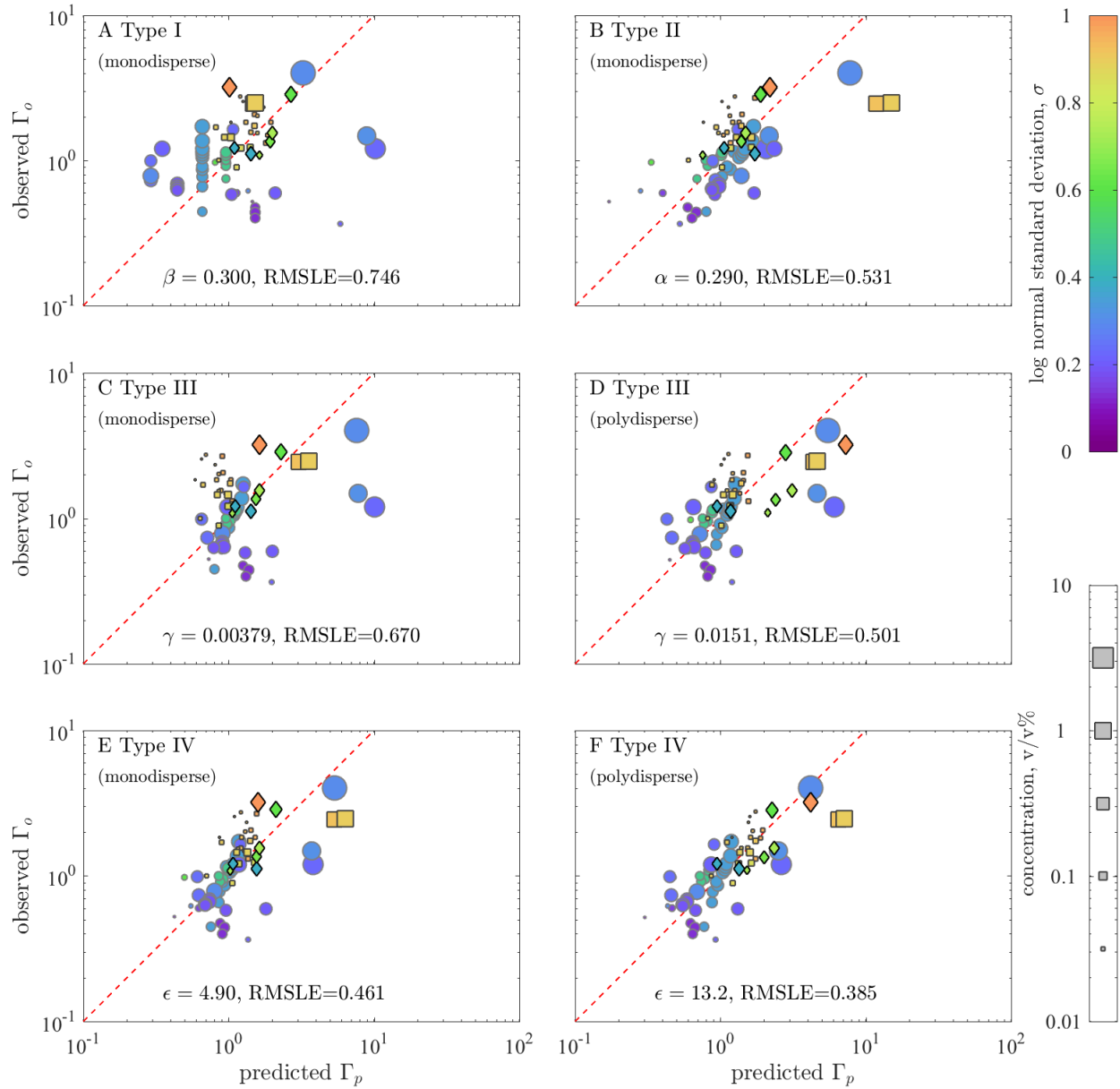


**Figure 2** Comparison of empirical and modeled net erosion-deposition thresholds. Plots show the observed,  $\Gamma_o$ , versus the predicted,  $\Gamma_p$ , dimensionless shear stress for: monodisperse models Types I (A), II (B) and III (C) and IV (E); and the polydisperse models III (D) and IV (F). Symbols are as in Figure 1, the dashed red line describes exact fit. The colors refer to the log normal standard deviation of particle-size,  $\sigma$ .

## 3.2 Net Erosion and Deposition Threshold Models

Existing models of the net erosional-depositional threshold are tested and compared against empirical observations. The goodness of fit between observed,  $\Gamma_o$ , and predicted,  $\Gamma_p$ , dimensionless shear stress (Figure 2), is given by the Root Mean Square Logarithmic Error (RMSLE) for which smaller numbers represent lower error. A new model is then proposed based on these comparisons.

### 3.2.1 Rouse Models

In competence based (Type I “Rouse”) models, deposition rate is an assumed function of flow stratification. As stratification scales with the settling to shear velocity ratio [*Soulsby, 1997*], some equilibrium flow models [*Komar, 1985; Kneller, 2003; Kubo et al., 2005; Lynds et al., 2014*] have assumed a net erosional-depositional threshold given by

$$(2) \quad w_s = \beta u_*$$

where  $w_s$  is the (particle size dependent) characteristic particle settling velocity (see Supporting Information) and  $\beta$  is an empirical Rouse parameter [*Rouse, 1937*]. Settling velocity is estimated based on the median particle diameter. Although alternative models have used different percentile particle sizes to characterize the settling velocity of sediment in suspension they may all be criticized as failing to describe the dynamics of the finer or coarser particle classes respectively [see *Komar, 1985* and references therein]. An iterative best fit of the theoretical model to data yields  $\beta=0.300$  and  $RMLSE=0.746$  (Figure 2a). The Rouse parameter describes a threshold between erosion and deposition independent of concentration or particle-size distribution. Regardless of whether the particle-size distribution can be ignored, the Rouse criterion must be fundamentally flawed as the threshold condition is known to be dependent on the concentration of

material in suspension [Garcia, 2008]. A corollary is that the commonly used transition criterion between bedload (transport dominated by particle-bed interaction) and suspended load (transport dominated by turbulent fluid motion),  $u_* = w_s$  [Soulsby, 1997] should also take concentration into account (see Supporting Information).

### 3.2.2 Flow Power Models

Capacity based (Type II “Flow Power”) models assume that when deposition and erosion are in balance the rate of work done keeping material in suspension,  $g\Delta\rho cw_s$ , is directly proportional to available flow power [Velikanov, 1954; Bagnold, 1966; Celik and Rodi, 1991; Garcia, 2008], that is proportional to  $\rho u_*^3/h$  [see Supporting Information; Pope, 2000; Wright and Parker, 2004]. The net erosional-depositional threshold is thus implicitly defined by

$$(3) \quad g\Delta\rho cw_s h = \alpha \rho u_*^3.$$

In equation (3)  $h$  is flow depth and  $\alpha$  is an empirical constant specifying the energy efficiency of the flow [Li et al., 2014; Bizzi and Lerner, 2015]. An iterative best fit of the theoretical model to data yields  $\alpha=0.290$  and  $\text{RMSLE}=0.531$  (Figure 2b). Although derivable from first principles (see Supporting Information), mechanistic flow power models do not offer a means to account for particle-size distribution or competence effects on threshold conditions.

### 3.2.3 Flux Balance Models

Alternatively, competence-capacity based (Type III “Flux Balance”) models equate the net rate of sediment entrainment from the bed to the net rate of deposition from suspended load [Smith and Hopkins, 1973; Garcia and Parker, 1991, 1993; Garcia, 2008], a formulation that can be traced back to the original morphodynamic models of Exner [Exner, 1920, 1925]. For a

polydisperse suspension of  $N$  distinct particle classes, individual,  $c_i$ , and sum,  $c = \sum_{i=1}^N c_i$ , particle class concentrations determine the criteria for threshold flow [Dorrell *et al.*, 2013], as given by the  $N + 1$  conditions

$$(4) \quad \frac{c_i^-}{c_m} E_i = c_i^+ w_{si} \quad \forall i \text{ and } \sum_{i=1}^N c_i^- = c_m.$$

Here the sediment entrainment rate is defined by  $E_i$ ; the packing concentration,  $c_m = 0.6$ , is assumed constant [Dorrell and Hogg, 2010]; particle class concentration near the bed, at height  $z^+ = 0.01h$  [Soulsby, 1997], is defined by  $c_i^+$ ; particle class concentration in the active layer of the bed, which freely exchanges material with material transported as suspended load [Dorrell *et al.*, 2013], is defined by  $c_i^-$ . Here particle distribution-dependent hiding effects in the active layer are assumed negligible [Wilcock and Southard, 1988] and the active layer is assumed to contain only particle classes also in suspension [Dorrell *et al.*, 2013]. Given the near bed concentration and sediment entrainment rate, the threshold condition is given by the minimum shear velocity that satisfies equation (4) where  $0 \leq c_i^- \leq c_m$ . Near bed concentration is proportional to individual capacity  $c_i^+ = c_i / \lambda_i$ ; assuming the flow is dilute and turbulence dampening is negligible [see, e.g., Smith and McLean, 1977; van Rijn, 1984a; Gelfenbaum and Smith 1986], the shear and particle settling velocity dependent stratification shape function,  $\lambda_i$ , is given by the depth averaged Rouse profile [see Supporting Information; Rouse, 1937].

Previous studies suggest that entrainment rate is a competence-limited function of forces applied to the bed, i.e. the available flow power above that required for incipient particle motion given by  $\Delta u_*^3 / h = \max(u_*^2 - u_{*ci}^2, 0)^{3/2} / h$  [van Rijn, 1984b] and the properties of the material being entrained [van Rijn, 1984b; Garcia and Parker, 1991 and 1993], i.e. particle-size,  $d_i$ . Here  $u_{*ci}$  is the critical shear velocity for incipient motion of a particle of given size. To close equation (4) a

common sediment entrainment function, based on erosional flow experiments [*van Rijn*, 1984b; *Dorrell et al.*, 2013; *Basani et al.*, 2014], is used that takes the form

$$(5) \quad E_i = \gamma \rho (g \Delta \rho d_i)^{-1} \Delta u_{*i}^3$$

( $\gamma$  being an empirical parameter describing entrainment efficiency). This particle-size dependent entrainment function is employed in current (Type III) models, equations (4)-(5). An iterative best fit of the monodisperse form of this model to data yields  $\gamma=3.79 \times 10^{-3}$  and a RMSLE=0.670 (Figure 2c). Using a polydisperse model to explicitly model size distribution improves the fit giving  $\gamma=1.51 \times 10^{-2}$  and a RMSLE=0.501 (Figure 2d).

### 3.2.4 Flow-Power Flux-Balance Model

In the limit of a monodisperse unstratified suspension, where deposition scales with  $cw_s$  [*Dorrell et al.*, 2013], the flow power model (3) implies that erosion of sediment scales with  $\rho u_*^3 / g \Delta \rho h$ . However, the flux balance model, equations (4)-(5), does not recover this mechanistic description of the flow. In the regime of an unstratified suspension,  $w_s \ll u_*$ , a series expansion of the flux-balance model (4)-(5) implies that equilibrium erosion (in balance with deposition) scales inversely with particle diameter,  $cw_s \propto \rho u_*^3 / (g \Delta \rho d)$ , to leading order.

This result motivates the development of a new flow-power, flux-balance (Type IV) model that: recovers the mechanistic flow power model  $cw_s \propto \rho u_*^3 / (g \Delta \rho h)$  of threshold flow, for  $w_s \ll u_*$ ; describes flow competence; and may be extended to describe polydisperse suspensions. This is achieved using a new sediment entrainment function for flow at the threshold between net erosion and net deposition. Here the power required to lift sediment into suspended load,  $g \Delta \rho E_i$ , is assumed proportional to the depth averaged available flow power,  $\rho \Delta u_*^3 / h$ . Whilst entrainment is limited by particle size dependent competence, the new entrainment function has the form

$$(6) \quad E_i = \varepsilon \rho (g \Delta \rho h)^{-1} \Delta u_{*i}^3,$$

which scales with flow depth, and is a key departure from existing entrainment models that are scaled using particle diameter ( $\varepsilon$  being an empirical parameter describing entrainment efficiency). This flow depth - dependent entrainment function is used to close the flow-power flux-balance (Type IV) model, equations (4) and (6). An iterative best fit of the monodisperse form of this model to empirical data yields  $\varepsilon=4.90$  and a RMSLE=0.461 (Figure 2c); the polydisperse form of this model improves the fit, where  $\varepsilon=13.2$  and a RMSLE=0.385 (Figure 2d). The improvement in threshold flow predictions by using a flow depth rather than particle diameter [*van Rijn, 1984b; Garcia and Parker, 1993*] scaled entrainment rate is also demonstrated by the decrease in RMSLE from 0.501 to 0.385 between the Type III and IV models (Figures 2d and f).

### 3.3 Reference Concentration

A reference concentration condition is often used to close modeled sediment in suspension [*Soulsby, 1997*]. As stressed by *Dorrell and Hogg (2011)*, such a boundary condition can only be applied at the threshold between net erosion and deposition, as its use in temporally or spatially evolving flows may result in erroneous gravitationally unstable profiles of suspended sediment concentration. The reference concentration may easily be determined from the flux balance models (Type III and IV) as the sum near-bed concentration,  $\sum_{i=1}^N c_i^+$ , see Figure 3. For example, assuming the capacity to transport particles in suspension is indeed related to flow power [*Velikanov, 1954; Bagnold, 1966*], the near bed reference concentration is shown from equations (4) and (6) to be a function of the composition of the active layer of the bed and particle size (settling velocity) distribution

$$(7) \quad \sum_{i=1}^N c_i^+ = \sum_{i=1}^N \varepsilon \frac{\rho}{(g \Delta \rho h)} \frac{c_i^-}{c_m} \frac{\Delta u_{*i}^3}{w_{si}} \quad \text{where} \quad \sum_{i=1}^N c_i^- = c_m.$$

Therefore, the near bed suspended load reference concentration must be particle size (settling velocity) dependent, given the balance between the work done keeping sediment in suspension and the available power of the flow. This contrasts with research that hypothesizes that near-bed concentration is particle size independent (for particles  $<200\mu\text{m}$  in diameter) [e.g., *Eggenhuisen et al.*, 2017]. More generally, the reference concentration is also dependent on the composition of the active layer,  $c_i$ . Thus, there is no unique solution for the suspended load capacity of a polydisperse suspension of particulate material at a given shear velocity [*Dorrell et al.*, 2013]. However, if the concentration, size distribution and the shear velocity dependence of the vertical distribution of material in suspension is known a unique solution for the shear velocity at the threshold between net deposition and erosion may be found using the flux balance models, Type III and IV (Figures 2 and 3).

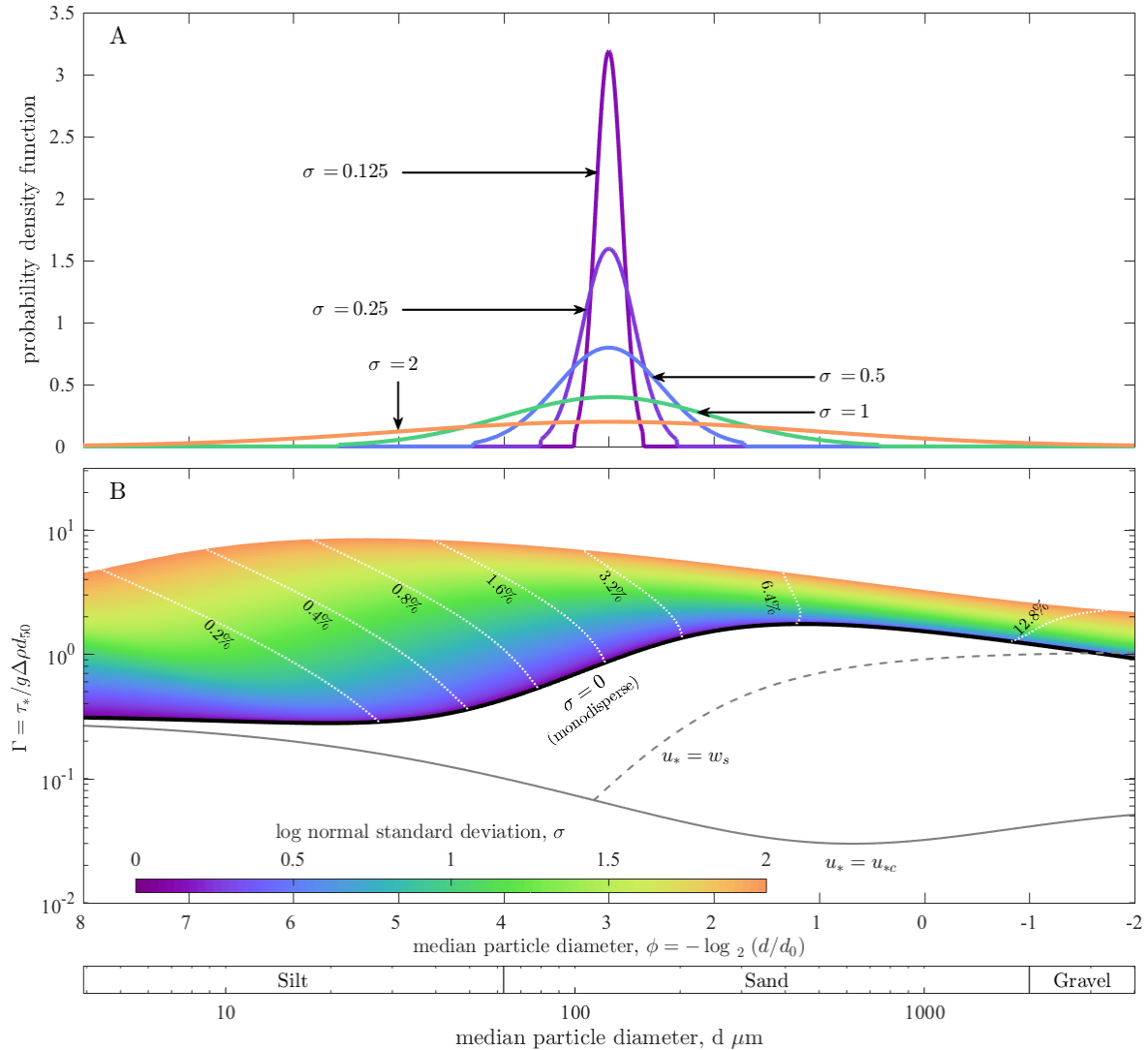


**Figure 3** Dependence of the dimensionless shear stress,  $\Gamma$ , on particle size standard deviation. (A) Log normal suspended load particle-size distributions, truncated to the central 99% range. (B) Threshold dimensionless shear stress,  $\Gamma$ , derived using the flux balance model (Type IV), at average empirical flow conditions ( $c = 0.1\%$  and  $h = 0.25\text{m}$  – see Supporting Data Table 1). Particle size distribution is specified *a priori* by a log-normal distribution, (A). The dotted white curves describe the near-bed reference concentration,  $\Sigma_{i=1}^N c_i^+$ . The solid gray curve denotes the Shields condition for incipient motion, whilst the dashed gray curve denotes the Rouse condition for suspended load transport.

## 4 Discussion

Comparing all the models discussed, monodisperse models in general provide a poorer collapse between the observed,  $\Gamma_o$ , and predicted,  $\Gamma_p$ , dimensionless shear (Figures 2a-c). The discretization of particle-size distribution improves model predictions; the polydisperse form of the new Type IV model, which uses the flow power based sediment entrainment formula, provides the best collapse (Figure 2f). Notably, where suspended particle-size distribution was explicitly recorded (i.e. the 30 experiments comprising the type A and B data), the Type IV model provides the best prediction of threshold between net-erosion deposition (compare Figures 2b and 2f). Fit of the type C data is also improved using the Type IV model, but this depends on the interpolated distribution of material in suspension (section 2.2). Moreover, discretization of the particle-size distribution significantly improves prediction of flow conditions recorded in laboratory and fluvial observations (compare Figures 2e and 2f). This is due to increasingly wider particle-size distributions enhancing vertical flow stratification and thus depositional flux. Consequently, the shear stress must increase for the flow to maintain the net erosional-depositional threshold. The effect of stratification is magnified by the non-linear dependence of settling velocity on particle size [S Soulsby, 1997].

As shown in Figure 3, the net erosion – deposition threshold for particulate laden flows at equilibrium occurs in the suspended load regime. In contrast to previous studies, where sediment transport was predicted using characteristic particle size [see, e.g., Velikanov, 1954; Bagnold, 1966; Celik and Rodi, 1991; Soulsby, 1997; Kubo et al., 2005; Yang, 2006; Bizzi and Lerner, 2015], the net erosion – deposition threshold is shown to also depend strongly on particle-size distribution (Figures 1 and 3). For example, the dimensionless shear stress required to maintain threshold

conditions for coarse silt ( $\phi=5$ ) increases by  $\sim 3,000\%$  when varying from monodisperse,  $\sigma=0$ , to poorly sorted [Folk, 1966],  $\sigma\approx 2$ , sediment (Figure 3b). In contrast changes in characteristic particle size have a comparatively small effect, with a maximum  $\sim 250\%$  increase in dimensionless shear stress for  $8\geq\phi\geq-2$  and  $\sigma=1$  (Figure 3b). Thus, particle-size distribution is a dominant control on the dimensionless shear stress at the threshold between net erosional and depositional flow; although, it is noted, from Figure 1, that characteristic particle size, and suspended load concentration, also affect this threshold. Moreover, this threshold also influences other critical sediment transport parameters including flow concentration (i.e., capacity) and in turn the maximum sediment transport flux per unit area (i.e., the product of flow concentration and velocity, which is proportional to shear stress). The order of magnitude variations in dimensionless shear stress with particle size distribution (Figure 3) may thus explain the large errors inherent in existing monodisperse sediment transport models [Yang, 2006].

As posed, sediment concentration, determined by stratification (2), flow power (3) or entrainment (5)-(6), increases with the amount of turbulent mixing characterized by shear velocity. However, with increasing volume concentration there is a non-linear relationship between the energy needed to keep material in suspension and flow power, since turbulence is progressively dampened with suspension of particulate material [Yang, 2006]. Thus, the threshold formulation, Equations (2)-(6), only holds for dilute flow, not for the sub- super saturated threshold of hyper-concentrated flows [van Maren *et al.*, 2009]. Transition to hyper-concentrated flow occurs across a wide range of concentrations,  $0.1 < c < 0.4$  [see van Maren *et al.*, (2009) and references therein]. Moreover, whilst we have proposed empirical closures scaling the dependence on shear velocity, further work is required to elucidate the physical processes controlling these scaling parameters.

Here we have shown that the effect of particle-size distribution on controlling the threshold between net erosion and net deposition from suspended load transport is far more important than has previously been recognized. Previous work may have overstated the predictive ability of monodisperse models as they have predominantly compared them to comparatively narrow particle-size distributions. Comparison to wider particle size distributions typical of many natural environments and industrial settings, demonstrates the limitations of these monodisperse models and the importance of particle sized distribution (Figure 3).

## **5 Conclusions**

Here it is shown that particle-size distribution is a dominant control on the threshold between net erosion and net deposition of suspended particles in environmental and industrial flows. Thus, polydisperse, rather than monodisperse, particle-size modeling approaches are required to predict the threshold between the entrainment and deposition of particulate material into suspended load. Broader particle-size distributions enhance suspended sediment stratification and thus the near-bed sediment concentration and depositional flux. Consequently, threshold conditions occur at higher shear stresses in flows carrying broader particle distributions compared with those carrying narrower distributions. Therefore, the threshold does not have unique values for specific combinations of flow concentration and characteristic particle size – implicit in existing theories – but has a range of possible values depending on particle-size distribution. To predict the threshold, a new sediment entrainment function is proposed based on the flow-power model of suspended load particle transport capacity. By doing so, suspended load polydispersity is incorporated, providing a better than order-of-magnitude improvement compared to existing models. The results also explain the wide variations observed in current models when the net erosional-depositional threshold is based on a characteristic particle size. This model establishes a

basis for accurate predictions of particle-laden flow hydro- and morpho-dynamics, applicable across a wide range of environmental, engineering and industrial settings.

## **Acknowledgments**

This work was supported by the Turbidites Research Group, University of Leeds, UK. We thank Alan Haywood, Jim Hendy, Nigel Mountney and Paul Wignall for helpful discussions and commenting on the initial manuscript. We thank David Mohrig and Joris Eggenhuisen for providing thought provoking reviews that have significantly improved the paper. Data used are detailed in the online supporting information.

## **References**

- Armanini, A. and G. Di Silvio (1988), A one-dimensional model for the transport of a sediment mixture in non-equilibrium conditions. *J. Hydraul. Res.* 26, 275-292.
- Ashida, K. and T. Okabe (1982), On the calculation method of the concentration of suspended sediment under non-equilibrium condition. In *Proceedings of the 26th Conference on Hydraulics*, 153-158.
- Bagnold, R. A. (1966), *An approach to the sediment transport problem*. Geol. Surv. Prof. Pap. 442-I, Washington, D.C.
- Basani, R., M. Janocko, M. J. Cartigny, E. W. Hansen, and J. T. Eggenhuisen, (2014). MassFLOW-3DTM as a simulation tool for turbidity currents?: some preliminary results. In *Depositional Systems to Sedimentary Successions on the Norwegian Continental Margin*,

- edited by Martinius, A. W., Ravnås, R., Howell, J. A., Steel, R. J., Wonham, J. P., Int. Assoc. Sedimentol. Spec. Publ., 46, 587-608.
- Bayat, H., M. Rastgo, M. M. Zadeh and H. Vereecken (2015), Particle size distribution models, their characteristics and fitting capability. *J. Hydrol.* 529, 872-889.
- Blom, A. and G. Parker (2004), Vertical sorting and the morphodynamics of bed form-dominated rivers: A modeling framework. *J. Geophys. Res. Earth Surf.* 109, F02007.
- Bizzi, S. and D. N. Lerner (2015), The use of stream power as an indicator of channel sensitivity to erosion and deposition processes. *River Res. Appl.* 31, 16-27.
- Brooks, N. H. (1954), Laboratory Studies of the Mechanics of Streams Flowing over a Movable Bed of Fine Sand, Doctoral dissertation, California Institute of Technology.
- Bufe, A., C. Paola, and D. W. Burbank, (2016) Fluvial bevelling of topography controlled by lateral channel mobility and uplift rate. *Nat. Geosci.* 9, 706-710.
- Cantero, M. I., A. Cantelli, C. Pirmez, S. Balachandar, D. Mohrig, T. A. Hickson, T. Yeh, H. Naruse and G. Parker (2012) Emplacement of massive turbidites linked to extinction of turbulence in turbidity currents. *Nat. Geosci.* 5, 42-45.
- Celik, I. and W. Rodi (1991), Suspended sediment-transport capacity for open channel flow. *J. Hydraul. Eng.* 117, 191-204.
- Cellino, M. and W. H. Graf (1999) Sediment-laden flow in open-channels under noncapacity and capacity conditions. *J. Hydraul. Eng.* 125, 455-462.
- Coleman, N. L. (1986), Effects of suspended sediment on the open-channel velocity distribution. *Water Resour. Res.* 22, 1377-1384.
- Dorrell, R. and A. J. Hogg (2010), Sedimentation of bidisperse suspensions. *Int. J. Multiph. Flow* 36, 481-490.

- Dorrell, R. M., and A. J. Hogg (2011), Length and time scales of response of sediment suspensions to changing flow conditions. *Journal of Hydraulic Engineering*, 138, 430-439.
- Dorrell, R. M., A. J. Hogg and D. Pritchard (2013), Polydisperse suspensions: Erosion, deposition, and flow capacity. *J. Geophys. Res. Earth Surf.* 118, 1939-1955.
- Einstein, H. A. and N. Chien (1955), Effects of Heavy Sediment Concentration Near the Bed on Velocity and Sediment Distribution. Missouri River Division, Corps of Engineers, US Army.
- Eggenhuisen, J. T., M. J. Cartigny, and J. de Leeuw (2017), Physical theory for near-bed turbulent particle suspension capacity. *Earth Surf. Dyn.*, 5, 269-281.
- Exner, F. M. (1920). Zur physik der dünen. *Hölder*.
- Exner, F. M. (1925). Über die wechselwirkung zwischen wasser und geschiebe in flüssen. *Akad. Wiss. Wien Math. Naturwiss. Klasse*, 134, 165-204.
- Folk, R. L. (1966), A review of grain-size parameters. *Sedimentology* 6, 73-93.
- Garcia, M. H. (2008), Sediment transport and morphodynamics, In: Garcia, M. H. (ed.), *Sedimentation Engineering: Processes, Measurements, Modeling and Practice*. ASCE Manuals and Reports on Engineering Practice No. 110. American Society of Civil Engineers, Reston, VA, 21–164.
- Garcia, M. H. and G. Parker (1991), Entrainment of bed sediment into suspension. *Journal of Hydraulic Engineering*, 117, 414-435.
- Garcia, M. H. and G. Parker (1993), Experiments on the entrainment of sediment into suspension by a dense bottom current. *J. Geophys. Res.* 98, 4793-4807.
- Gelfenbaum, G. and J. D. Smith (1986), Experimental Evaluation of a Generalized Suspended-Sediment Transport Theory. In *Shelf Sands and Sandstones*, edited by Knight, R. J. and S. R. McLean, Canadian Society of Petroleum Geologists, 133–144.

- Graf, W. H. and M. Cellino (2002), Suspension flows in open channels; experimental study. *J. Hydraul. Res.* 40, 435-447.
- Guy, H. P., D. B. Simons, and E. V. Richardson (1966), Summary of alluvial channel data from flume experiments, 1956-61. *US Geol. Surv. Prof. Pap.* 462-I.
- Halsey, T. C., A. Kumar, and M. M. Perillo (2017). Sedimentological regimes for turbidity currents: Depth-averaged theory. *J. Geophys. Res. Oceans*, 122, 5260-5285.
- Houssais, M., C. P. Ortiz, D. J. Durian and D. J. Jerolmack (2015), Onset of sediment transport is a continuous transition driven by fluid shear and granular creep. *Nat. Commun.* 6, 1-8.
- Kneller, B. (2003), The influence of flow parameters on turbidite slope channel architecture. *Marine and Petroleum Geology* 20, 901-910.
- Komar, P. D. (1985), The hydraulic interpretation of turbidites from their grain sizes and sedimentary structures. *Sedimentology* 32, 395-407.
- Kubo, Y. S., J. P. Syvitski, E. W. Hutton and C. Paola (2005), Advance and application of the stratigraphic simulation model 2D-SedFlux: From tank experiment to geological scale simulation. *Sediment. Geol.* 178, 187-195.
- Li, W., D. S. van Maren, Z. B. Wang, H. J. de Vriend and B. Wu (2014), Peak discharge increase in hyperconcentrated floods. *Adv. Water Resour.* 67, 65-77.
- Lyn, D. A. (1988), A similarity approach to turbulent sediment-laden flows in open channels. *Journal of Fluid Mech.* 193, 1-26.
- Lynds, R. M., D. Mohrig, E.A., Hajek and P. L. Heller (2014), Paleoslope reconstruction in sandy suspended-load dominated rivers. *Journal of Sedimentary Research* 84, 825–836.
- Nittrouer, J. A., D. Mohrig, and M. Allison, (2011). Punctuated sand transport in the lowermost Mississippi River. *J. Geophys. Res. Earth Surf.*, 116, F04025.

- Nittrouer, J. A., J. L. Best, C. Brantley, R. W. Cash, M. Czapiga, P. Kumar and G. Parker (2012), Mitigating land loss in coastal Louisiana by controlled diversion of Mississippi River sand. *Nat. Geosci.* 5, 534-537.
- Nordin, C. F. and G. R. Dempster (1963), Vertical distribution of velocity and suspended sediment, Middle Rio Grande, New Mexico, US Geol. Surv. Prof. Pap. 462-B.
- McLean, S. R. (1991), Depth-integrated suspended-load calculations. *Journal of Hydraulic Engineering*, 117, 1440-1458.
- McLean, S. R. (1992), On the calculation of suspended load for noncohesive sediments. *Journal of Geophysical Research: Oceans*, 97, 5759-5770.
- Parsi, M., K. Najmi, F. Najafifard, S. Hassani, B. S. McLaury and S. A. Shirazia (2014), A comprehensive review of solid particle erosion modeling for oil and gas wells and pipelines applications. *J. Nat. Gas Sci. Eng.* 21, 850-873.
- Pope, S. B. (2000), *Turbulent Flows*, Cambridge University Press, Cambridge, UK.
- Powell, M. J. D. (1964), An efficient method for finding the minimum of a function of several variables without calculating derivatives. *Comput. J.* 7, 155–162.
- van Rijn, L. C. (1984a), Sediment transport, part II: suspended load transport. *J. Hydraul. Eng.* 110, 1613-1641.
- van Rijn, L. C. (1984b), Sediment pick-up functions. *J. Hydraul. Eng.* 110, 1494-1502.
- Rouse, H. (1937), Modern conceptions of the mechanics of fluid turbulence. *Trans. Am. Soc. Civ. Eng.* 102, 463-505.
- Sajeesh, P. and A. K. Sen (2014), Particle separation and sorting in microfluidic devices: a review. *Microfluid. Nanofluidics* 17, 1-52.

- Shields, A. (1936), Anwendung der Aehnlichkeitsmechanik und der Turbulenzforschung auf die Geschiebebewegung. Preussischen Versuchsanstalt für Wasserbau, Berlin.
- Smith, J. D., and T. S. Hopkins (1973), Sediment transport on the continental shelf off of Washington and Oregon in light of recent current measurements. In Shelf Sediment Transport: Process and Patterns, edited by D. J. P. Swift, D. B. Duane, and O. H. Pilkey. 143-179, Hutchinson and Ross, Stroudsburg, Pa.
- Smith J. D. and S. R. McLean (1977), Spatially averaged flow over a wavy surface. Journal of Geophysical Research, 82, 1735-1746.
- Soulsby, R. (1997), Dynamics of Marine Sands: A Manual for Practical Applications. Thomas Telford Publications, UK.
- Strauss, M. and M. E. Glinsky (2012), Turbidity current flow over an erodible obstacle and phases of sediment wave generation. J. Geophys. Res. Oceans, 117, C06007.
- Syvitski, J. P., S. D. Peckham, R. Hilberman and T. Mulder (2003), Predicting the terrestrial flux of sediment to the global ocean: a planetary perspective. Sediment. Geol. 162, 5-24.
- Vanoni, V. A. (1946), Transportation of suspended sediment by water. Trans. Am. Soc. Civ. Eng. 111, 67-102.
- Vanoni, V. A. and G. N. Nomicos (1960), Resistance properties of sediment-laden streams. Trans. Am. Soc. Civ. Eng. 125, 1140-1167.
- van Maren, D. S., Winterwerp, J. C., Wang, Z. Y., and Pu, Q. (2009), Suspended sediment dynamics and morphodynamics in the Yellow River, China. Sedimentology, 56, 785-806.
- Velikanov, M.A. (1954), Gravitational theory of sediment transport. J. Sci. Sov. Union Geophys. 4.

- Walling, D. E. (2009), *The Impact of Global Change on Erosion and Sediment Transport by Rivers: Current Progress and Future Challenges*. UNESCO.
- Wang, S., S. Wang, B. Fu, S. Piao, Y. Lü, P. Ciais, X. Feng and Y. Wang (2015), Reduced sediment transport in the Yellow River due to anthropogenic changes. *Nat. Geosci.* 9, 38-42.
- Whitehouse, R. (1995), Observations of the boundary layer characteristics and the suspension of sand at a tidal site. *Cont. Shelf Res.* 15, 1549-1567.
- Wilcock, P. R. and J. B. Southard (1988) Experimental study of incipient motion in mixed-size sediment. *Water Resour. Res.* 24, 1137-1151.
- Wright, S. and G. Parker (2004), Flow resistance and suspended load in sand-bed rivers: simplified stratification model. *J. Hydraul. Eng.* 130, 796-805.
- Yang, C. T. (2006), *Erosion and Sedimentation Manual*. US Department of the Interior, Bureau of Reclamation, Denver, CO.